

# **An Experimental Technique for Quadrupole-Free Energy Ramping an IH-DTL**

Olivier Shelbaya

TRIUMF

**Abstract:** TRANSOPTR simulations of the separated function ISAC drift tube linac (DTL) have revealed an interesting configuration: accelerated beam transmitted without using quadrupoles. This configuration and its underlying beam dynamics is presented and discussed. From this, a novel DTL tank phasing strategy is introduced, in which operators power off all DTL and HEBT quadrupoles prior to changing the energy of the machine. Tank voltages are model computed using a previously recorded beam calibration. Using a modified DTL injection tune, which couples optimum cavity phasing with beam transmission through sections of the machine, operators tune cavity phases to maximize beam on a few Faraday cups, thereby implicitly setting the energy. The quadrupoles are powered on and tuned after this is completed for all tanks, requiring a single intervention.

## 1 Introduction

This document proposes a novel manner in which the longitudinal tune of the ISAC DTL IH cavities can be defined by an operator, without using transverse focussing from magnetic quadrupoles. The inherent procedural complexity associated with transverse DTL tuning during energy changes is a consequence of the magnetic component of the Lorentz force law:

$$\vec{F} = q(\vec{v} \times \vec{B})$$

Transverse quadrupole focussing fields ( $\vec{B}$ ) produce a velocity dependent optics. During initial setup, the machine is progressively ramped from zero to full desired energy gain. Presently, this procedure calls for an operator to monitor output beam energy and energy spread on a downstream diagnostic, following a dipole. This generates the need to periodically adjust the entire transverse tune to maintain transmission and therefore observable beam to work with.

To this day, strategies for mitigating the time and complexity of this operation have relied upon the establishment and cataloging of manually established tunes (transverse and longitudinal) at a variety of conditions, for example the maximum acceleration of each tank. However, reliance upon these tunes and techniques creates an issue: on-line tuning is no longer a product of modelling and simulation, but rather a procedural task, aiming to carefully reproduce a previously and empirically established state. Tuning becomes reactive as opposed to proactive.

Having now built a model of the DTL in TRANSOPTR [1, 2], it should in principle be possible to compute and re-compute transverse tunes at different machine configurations. But in the case of an energy ramp, this operation seems wasteful if it is only intended for what is a transient state of the linac.

This led me to call into question the paradigm of ISAC-DTL energy changes as a whole. Why bother monitor the energy as it is being ramped, if that introduces the need for a transport tune, which must then in turn be adjusted along with the cavities? All we really care about is to confirm the final state of the machine. If the need to adjust a transverse tune is removed, so is much of the procedural overhead. Can we exploit our understanding of beam optics and the dynamics of IH cavities to be both lazy and efficient?

## 2 Beam Dynamics of IH Cavities

In [3], Baartman introduces a potential description for radially symmetric, time dependent accelerating electric fields. This parametrization is incredibly convenient since it only depends on the one-dimensional intensity of the on-axis electric field, obtainable through either RF measurements or simulations, in addition to a handful of cavity parameters. For the field, all that is needed is a two column dataset relating the position and longitudinal intensity. This allows for IH cavity simulations in TRANSOPTR [2]. The F-matrix for such a case is:

$$\mathbf{F}(s) = \begin{pmatrix} 0 & \frac{1}{P_0} & 0 & 0 & 0 & 0 \\ \mathcal{A}(s) & 0 & 0 & 0 & 0 & 0 \\ 0 & 0 & 0 & \frac{1}{P_0} & 0 & 0 \\ 0 & 0 & \mathcal{A}(s) & 0 & 0 & 0 \\ 0 & 0 & 0 & 0 & \frac{\beta'}{\beta} & \frac{1}{\gamma^2 P_0} \\ 0 & 0 & 0 & 0 & \mathcal{B}(s) & -\frac{\beta'}{\beta} \end{pmatrix} \quad (1)$$

where:

$$\mathcal{A}(s) = -\frac{q}{2\beta c} \left( \mathcal{E}'(s)C - \mathcal{E}(s)S \frac{\omega\beta}{c} \right) \quad (2)$$

$$\mathcal{B}(s) = \frac{q\mathcal{E}(s)\omega S}{\beta^2 c^2}. \quad (3)$$

with the notation  $S = \sin(\omega t(s) + \theta)$  and  $C = \cos(\omega t(s) + \theta)$ . Here, the normalized magnitude of the on-axis electric field is noted  $\mathcal{E}(s)$ , whose image is bounded to  $[-1,1]$ . A dimensionless scaling parameter  $V_s$  allows us to control the field amplitude, while a phase parameter  $\phi_0$  changes the field's initial timing. Energy gain is then:

$$E(V_s, \phi) = E_0 + qV_s \int_0^L \mathcal{E}(s) \cos(\omega t(s) + \phi_0) ds, \quad (4)$$

for a field  $\mathcal{E}(s)$  of total length  $L$ , oscillating at a frequency  $\omega = 2\pi f$ . Inspection of the F-matrix allows us to identify  $\mathcal{A}(s)$  as the radial RF (de)focussing term, which depends both upon the field and its s-derivative. The function  $\mathcal{B}(s)$  is likewise involved in longitudinal (de)bunching.

The IH cavity fields of the DTL are known to produce narrow optimum solutions in  $(V_s, \phi)$  configuration space for each tank and buncher [4]. At a given voltage, only a very narrow range of phases will efficiently cause energy gain, while also minimizing longitudinal momentum spread. However, the analysis in [4] only concerned itself with the longitudinal components of the beam. No attention was given to the transverse tune or behavior.

Implementation of sequential tune optimization for TRANSOPTR [5, 6] has allowed for the automation of DTL tune computations. Simulations of sequential DTL tuning in TRANSOPTR have revealed, it should be pointed out accidentally, an interesting configuration: with all DTL quadrupoles unpowered, there are injected beam solutions that should transmit the machine. Such a state is shown in Figure 1.

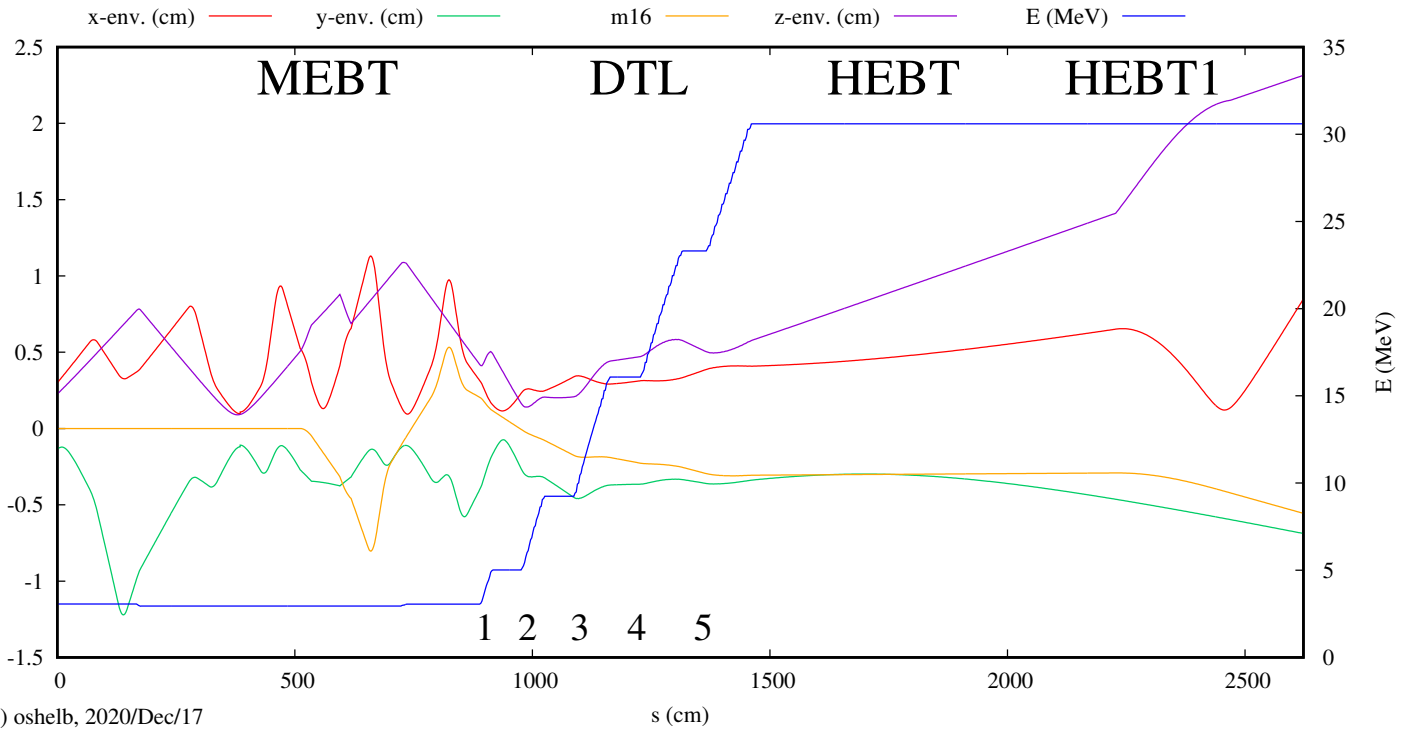


Figure 1: TRANSOPTR simulation of full ISAC-DTL acceleration, using only IH tanks 1 to 5, using no quadrupoles in either DTL or HEBT sections. DTL Injection has been computed so that the fully accelerated 2rms beam envelope remains smaller than the IH tube apertures through the machine. Locations of DTL IH-Cavities are labeled at the bottom of the plot. Energy (blue) is shown on the right-y axis, all others to the left y-axis.

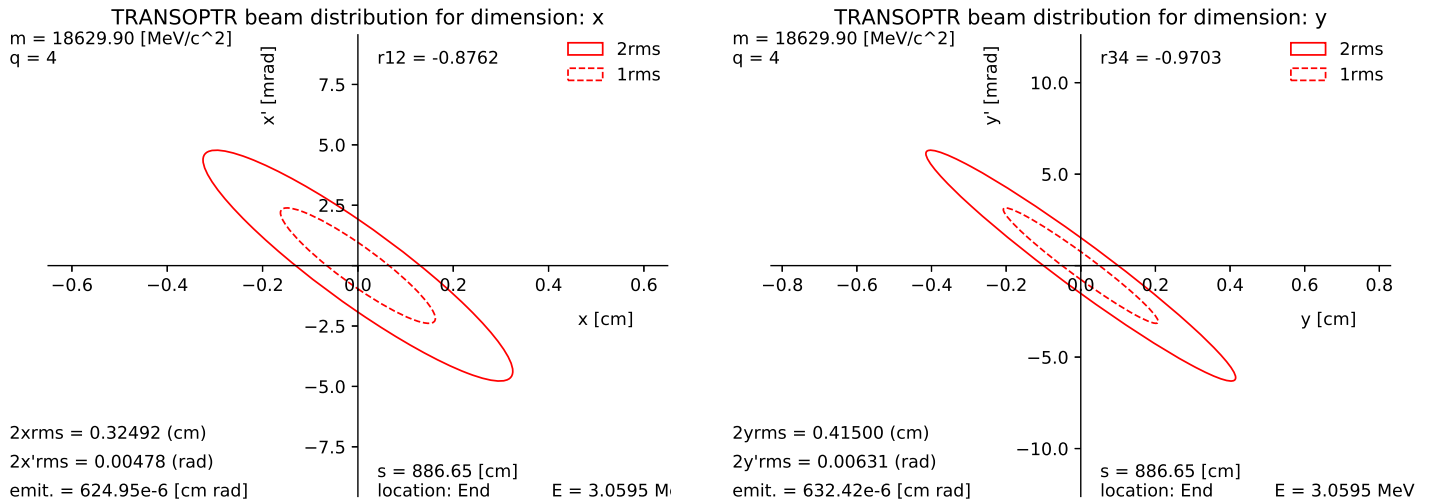


Figure 2: twissify generated transverse beam distribution at DTL:FC0, configured for quadrupole-free acceleration. The longitudinal distribution is time focussed into DTL Tank-1, using the MEBT rebuncher.

### 3 Optimum Energy Gain

For values of  $(V_s, \phi_0)$  where the integral (4) is maximized, we are only interested in solutions which minimize the energy spread, which will avoid excessive longitudinal bunch growth downstream of the accelerator. Using the TRANSOPTR model, whose parameters  $V_s$  have been calibrated with beam in [2], it is possible to find the optimum voltage and phase for each IH cavity, as was done in Fig. 1. This produces a model state of the linac, involving values of  $(V_s, \phi_0)$  which produce the desired acceleration.

However, while the voltage parameter should correspond to the control system voltage, the phase parameter will not. This is not only a matter of calibration; one must also consider that RF degrees in the current control system are not fixed to a master reference clock. During system reboots or other communication interruptions, the phasing parameters references may change, in such a way that manual cavity re-phasing is necessary.

With the DTL quadrupoles off and an injection distribution as noted in Figure 2, this can be overcome and actually exploited: for a given  $V_s$ , the phase  $\phi_0$  which maximizes energy gain also minimizes transverse divergence, causing maximum transmission to a sufficiently faraway Faraday cup. The tune shown in Figure 1 has been computed to cause the transverse envelope to be below the IH drift tube apertures when optimum acceleration takes place. In addition, the z-length is kept well below  $\beta\lambda$  in the DTL.

This allows an operator to set the pre-computed voltage, insert a Faraday cup downstream and by scanning only the cavity phase to maximize transmission, the energy is implicitly set. Once this is complete, the next IH cavity is powered on and the process repeated, until the desired energy is reached. At this point, the transverse tune can be defined, either manually or via model. Considering the behavior of the transfer matrix helps to understand how this procedure works. Recalling that the transfer matrix relates to the F-matrix and the potentials via:

$$\frac{d\mathcal{M}}{ds} = F\mathcal{M} \quad (5)$$

For a given voltage scaling  $V_s$ , the optimum phase is that for which the cumulative transfer matrix elements  $\mathcal{M}_{21}$ ,  $\mathcal{M}_{43}$  and  $\mathcal{M}_{65}$  are minimized in transit through the cavity. This occurs when the forces acting upon the bunch are minimized, though for nonzero net energy gain. In a manner of speaking, the optimum phase produces the gentlest possible path through the cavity, at a given  $V_s$ . The above three elements of  $\mathcal{M}$  are shown in Figure 3 for Tank-1 at a variety of phases, for a fixed  $V_s$  corresponding to maximum allowable tank voltage. Accordingly, we impose the following fit constraints upon the transfer matrix in TRANSOPTR:

$$\begin{aligned} \mathcal{M}_{21} &\rightarrow 0 \\ \mathcal{M}_{43} &\rightarrow 0 \\ \mathcal{M}_{65} &\rightarrow 0 \end{aligned}$$

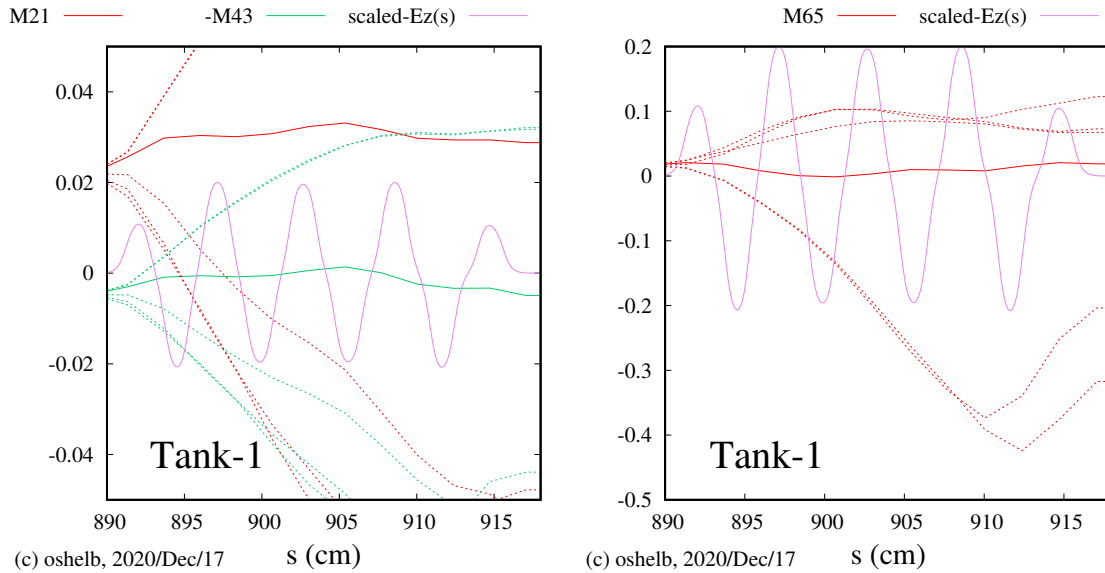


Figure 3: TRANSOPTR computed cumulative transfer matrix elements for the transverse (**Left**) and longitudinal (**Right**) cases, for the tune shown in Figure 1. In both plots, the optimum phase solution is shown as a solid line, corresponding to full acceleration and minimized forces acting upon the bunch. As the phase is scanned away from the optimum (dotted lines), the transfer matrix elements rapidly change value. The normalized Tank-1 longitudinal field  $\mathcal{E}(s)$  is superimposed for reference.

We note that in this case, the simulation is started at a longitudinal beam waist. Following the established procedure in [6], the database tags which encode this information are placed in sequence dtl\_db0.xml following each tank. As an example, the tag for Tank-1 is shown below:

```
<element id="mcat" type="fortline" s="332.0*mm" l="0">
<notes>tank-1 energy setting</notes>
<optr>! MCAT-verb: set-dtl-tank1-energy</optr>
<optr>!nlines: 6</optr>
<optr>!call fit(2,6,5,0.,1.,1)</optr>
<optr>!call fit(2,2,1,0.,1.,1)</optr>
<optr>!call fit(2,4,3,0.,1.,1)</optr>
<optr>!energerr0=0.251*mass - energk</optr>
<optr>!call fitarb(0.0,energerr0,1.,1)</optr>
<optr>! return</optr>
</element>
```

At each step, the cavity amplitude and phase are found with TRANSOPTR's internal optimizer, using simulated annealing [7]. Observe that DTL Tank-1 energy has been set here to the operational value for DTL Buncher-1 output energy, allowing us to skip buncher-1 use for full acceleration. At  $E/A = 1.53$  MeV/u, the same is found to be true for bunchers 2 and 3.

## 4 Procedure

The TRANSOPTR model is used to compute an injection tune for the MEBT section as previously shown in Figure 1. This will include voltage setpoints for all IH cavities, meaning the operator will have to ramp each cavity's voltage manually. In sequence, after establishment of a standard MEBT tune:

1. A standard unaccelerated pilot beam tune through the DTL is established.
2. The MEBT rebuncher is set for  $E/A = 0.153$  MeV/u and a z (time) focus is set at DTL Tank-1.
3. The MCAT-computed values for quadrupole-free injection are loaded to MEBT:Q11, Q12 and Q13.
4. All DTL and HEBT quadrupoles Q1 to Q8 are powered off. Beam is parked at MEBT:FC5.

(while output-E < desired-E):

- i Tank-n voltage is ramped by the operator to the MCAT computed value. The phase is not touched.
- i+1 MEBT:FC5 retracted, beam injected into the DTL. The operator then looks at a downstream Faraday cup while scanning Tank-n phase to maximize readable beam current. Figures 4, 5 and 6 list the terminal downstream cups for each tank. See appendix A for simulations of this. Note that for tanks 1, 2 and 3 it may be necessary to record a few phases which maximize transmission on the specified cup. If this is the case, refer to the appendix - one of the peaks will be the optimum accelerating phase, while the others will not. Upon powering on the next IH cavity, if the transmission remains poor, try the other recorded cavity phases. This exploits the fact that each IH cavity expects a given input energy - only one of the phases will then allow transmission.

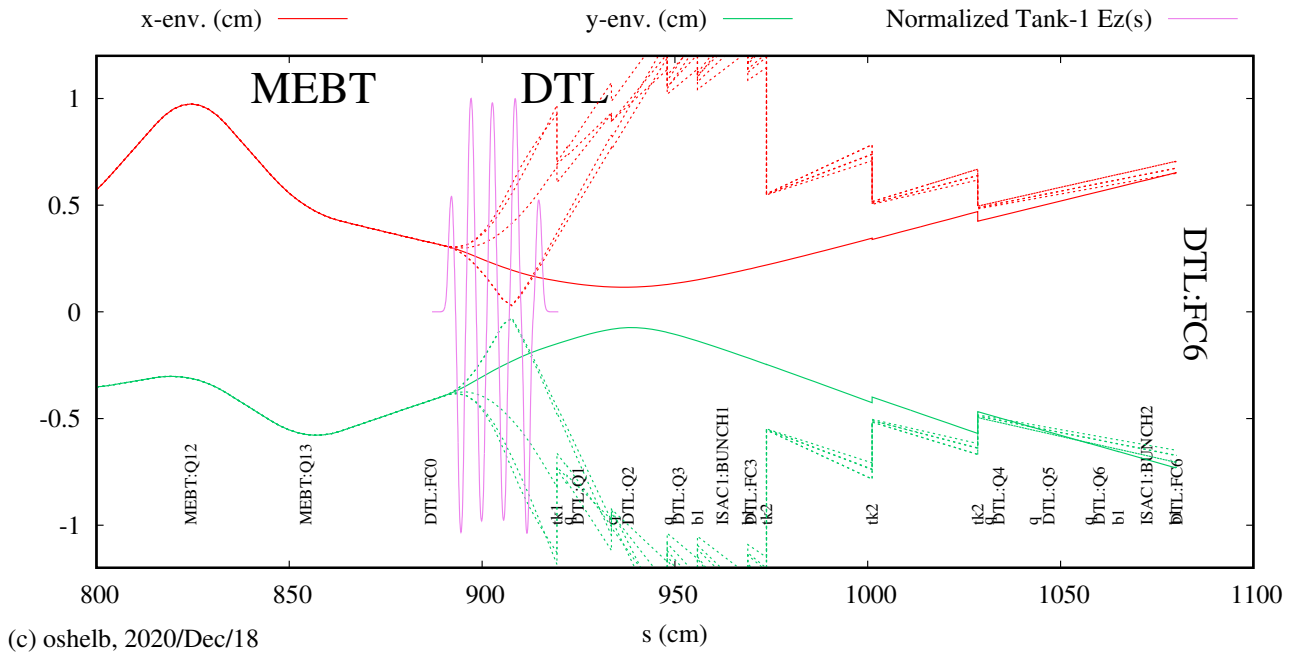


Figure 4: TRANSOPTR simulation of IH Tank-1 full/optimum acceleration (solid). A variety of transverse envelopes, suffering from a varying degree of transmission losses, are shown as dotted lines. The optimum phase minimizes these losses on DTL:FC6. The normalized on-axis electric field  $\mathcal{E}(s)$  is shown for reference. The subroutine SLIT [8] has been used at the entrance of downstream elements to simulate beamline aperture constraints.

Geometric constraints in the beamline include drift tube apertures of variable sizes (see [2] for details) and quadrupole aperture diameters of roughly 1". The phase versus transmission profile for each cavity is unique at a given  $V_s$ . See Appendix A for IH cavity parameter space scans on downstream Faraday cups. This phase to transmission response can easily be measured.

Figures 4, 5 and 6 show the change in transverse beam envelopes as the phase is shifted away from optimum acceleration. This will generate considerable losses within the structure, allowing the operator to exploit the strong correlation between transmission and beam energy using the cavity phase.

For a full energy ramp, all DTL IH tanks are set in the same way as Tank-1. In the case of Tanks 2 and 3, HEBT:FC0 should be sufficiently far, while for Tanks 4 and 5 the operator may wish to work at HEBT:FC5. At the end of the procedure, the longitudinal tune of the DTL is set.



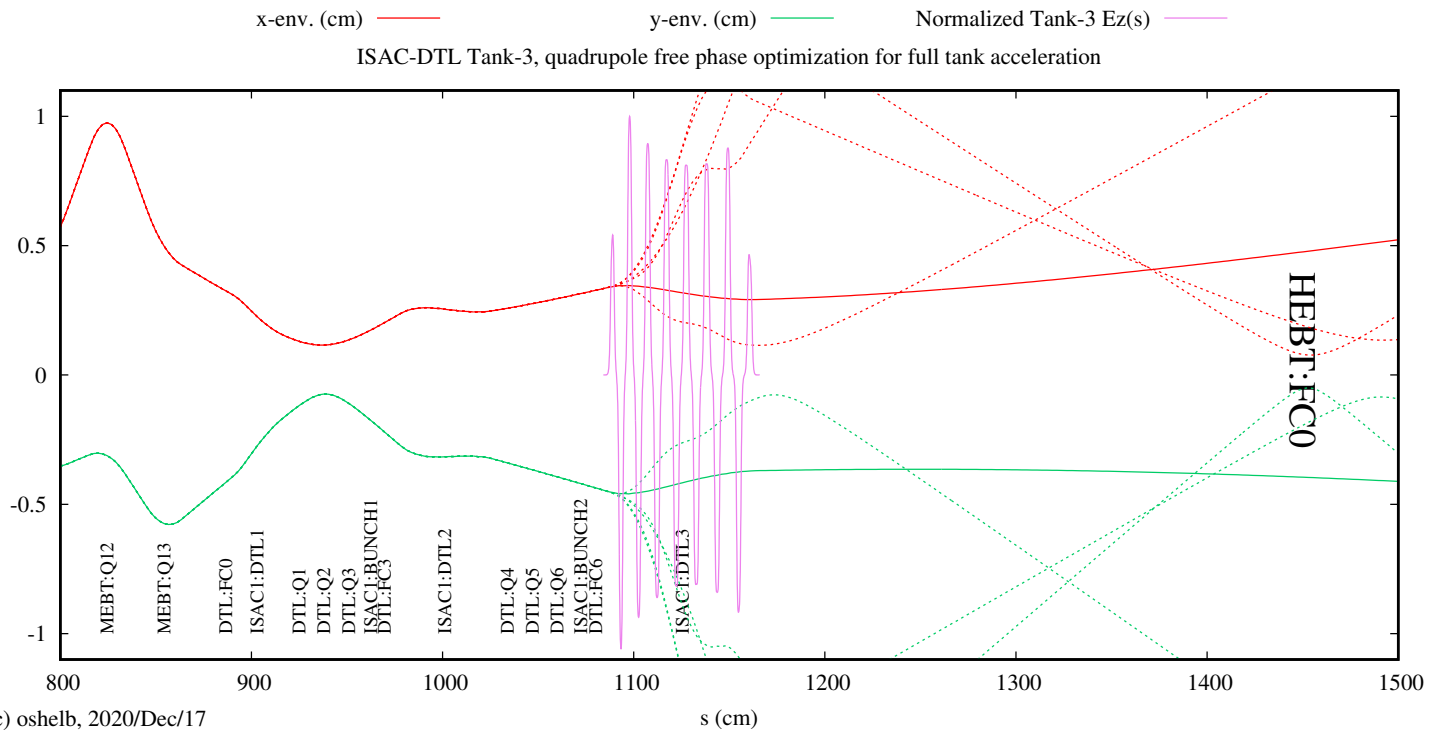
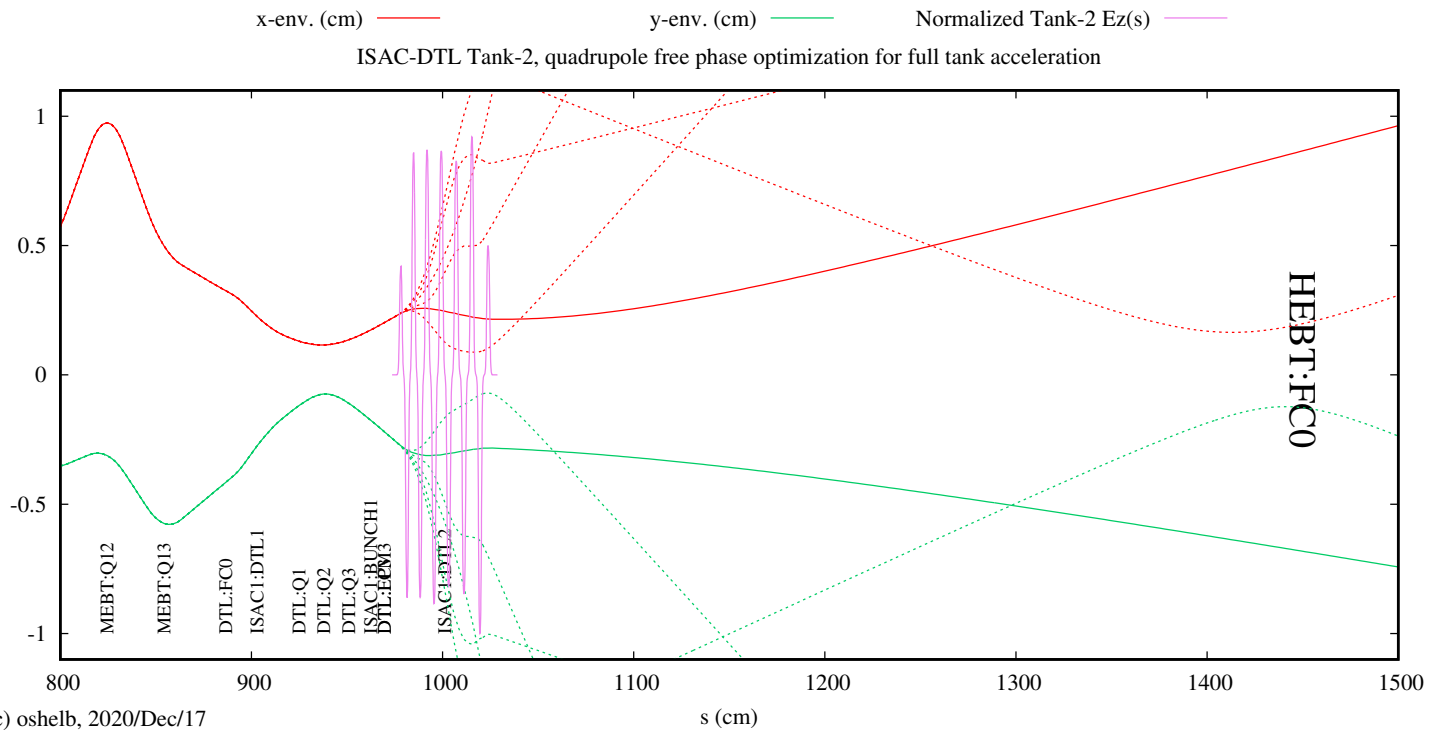


Figure 5: TRANSOPTR simulation of IH Tank-2 (**Top**) and Tank-3 (**Bottom**) full/optimum acceleration (solid). A variety of transverse envelopes, suffering from a varying degree of transmission losses, are shown as dotted lines. The optimum phase minimizes these losses on HEBT:FC0. The normalized on-axis electric field  $\mathcal{E}(s)$  is shown for reference. Note DTL IH tube radii are below 1cm.

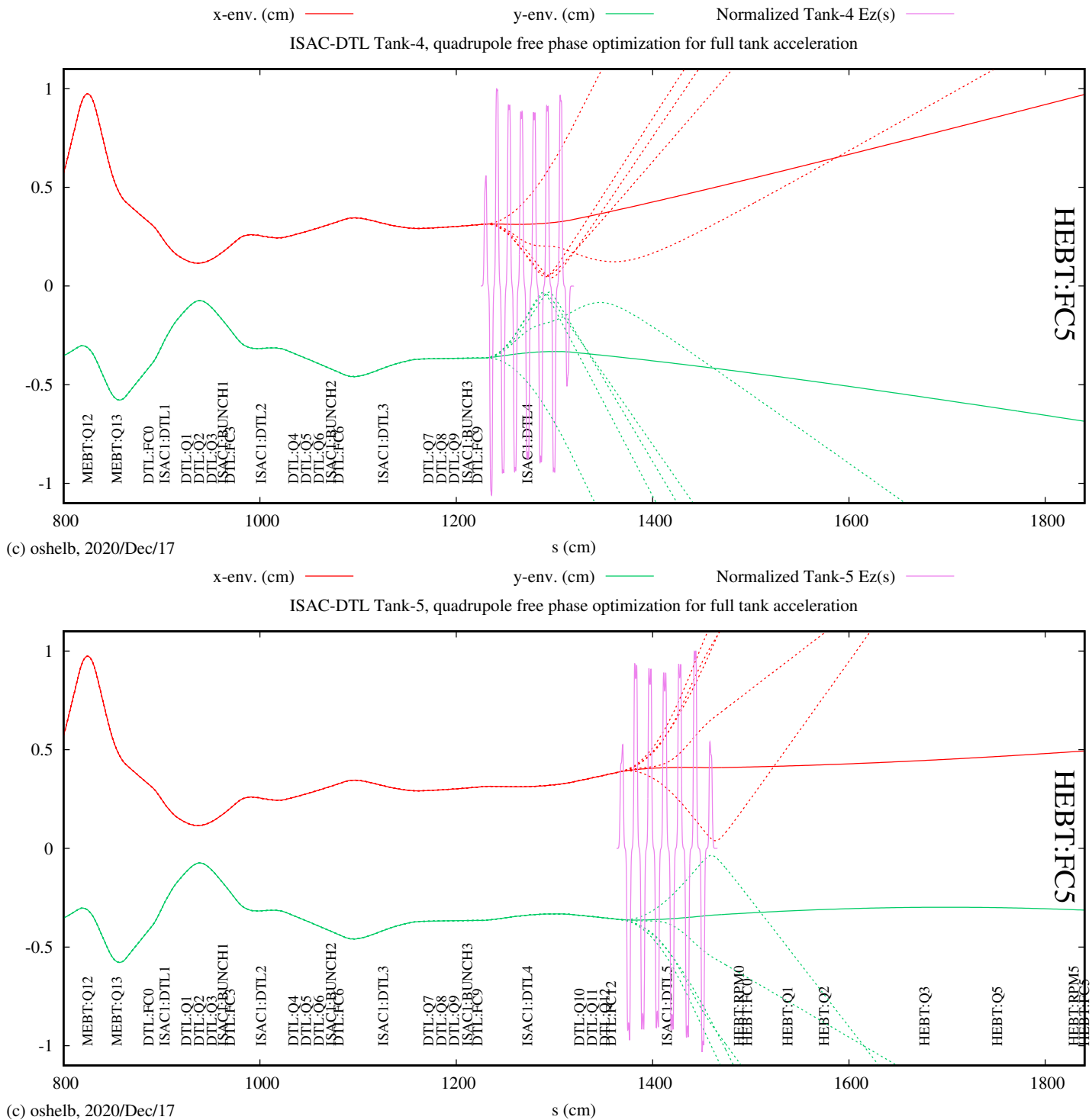


Figure 6: TRANSOPT simulation of IH Tank-4 (**Top**) and Tank-5 (**Bottom**) full/optimum acceleration (solid). A variety of transverse envelopes, suffering from a varying degree of transmission losses, are shown as dotted lines. The optimum phase minimizes these losses on DTL:FC6. The normalized on-axis electric field  $\mathcal{E}(s)$  is shown for reference.

## 5 Conclusion

The quadrupole-free DTL configuration shown herein possesses the interesting property that its transmission is very strongly tied to the setting of cavity voltage and phase parameters which result in cavity energy gain with minimized effect upon the bunch distribution. This tune should allow operators to perform rapid DTL energy changes using only a handful of DTL Faraday cup readings to infer proper acceleration. Removing the reliance upon a velocity dependent transverse tune, which must itself be maintained and optimized during the procedure considerably simplifies the process. This procedure, only simulated in TRANSOPTR to date, will be tested on-line for verification.

As an additional visualization of this machine configuration, a series of `topology.py` scans [5] have been performed for each IH tank in the DTL. These are shown in Appendix A, along with a brief description. The  $(x,y)$  envelopes are shown at the top of each figure, while the inverted value of  $P_z$  and the energy are shown at the bottom.

It is noted that the observation of multiple degenerate transmission peaks for certain cavities and the necessity to record them for testing with a downstream cavity adds to the complexity of this procedure. This step is attributable to the unfixed nature of the software phasing in the present system. If a master phasing value can be achieved in EPICS, which would remain unchanging across control system reboots or interruptions, then a calibration could be established, removing the need for this step. Instead, an operator could scan about an expected phase range.

## References

- [1] Heighway EA and Hutcheon RM. *Transoptr - A second order beam transport design code with optimization and constraints*. Technical report, Atomic Energy of Canada Limited, 1981.
- [2] Olivier Shelbaya. The TRANSOPTR Model of the ISAC Drift Tube Linear Accelerator - Part I: Longitudinal Verification. Technical Report TRI-BN-20-08, TRIUMF, 2020.
- [3] Richard Baartman. Linac Envelope Optics. Technical Report TRI-BN-15-03, TRIUMF, 2015.
- [4] Olivier Shelbaya. Nonlinear RF Cavities. Technical Report TRI-BN-20-05, TRIUMF, 2020.
- [5] Olivier Shelbaya. Longitudinal Beam Topology with TRANSOPTR. Technical Report TRI-BN-20-01, TRIUMF, 2020.
- [6] Olivier Shelbaya. Sequential Tune Optimization with TRANSOPTR. Technical Report TRI-BN-20-14, TRIUMF, 2020.
- [7] Richard Baartman. TRANSOPTR: Changes since 1984. Technical Report TRI-BN-16-06, TRIUMF, 2016.
- [8] Richard Baartman. SLIT routine for TRANSOPTR. Technical Report TRI-BN-19-21, TRIUMF, 2019.

# Appendices

## A IH Cavity ( $V_s, \phi_0$ ) Configuration Space Scans in TRANSOPTR (All DTL/HEBT Quadrupoles Off)

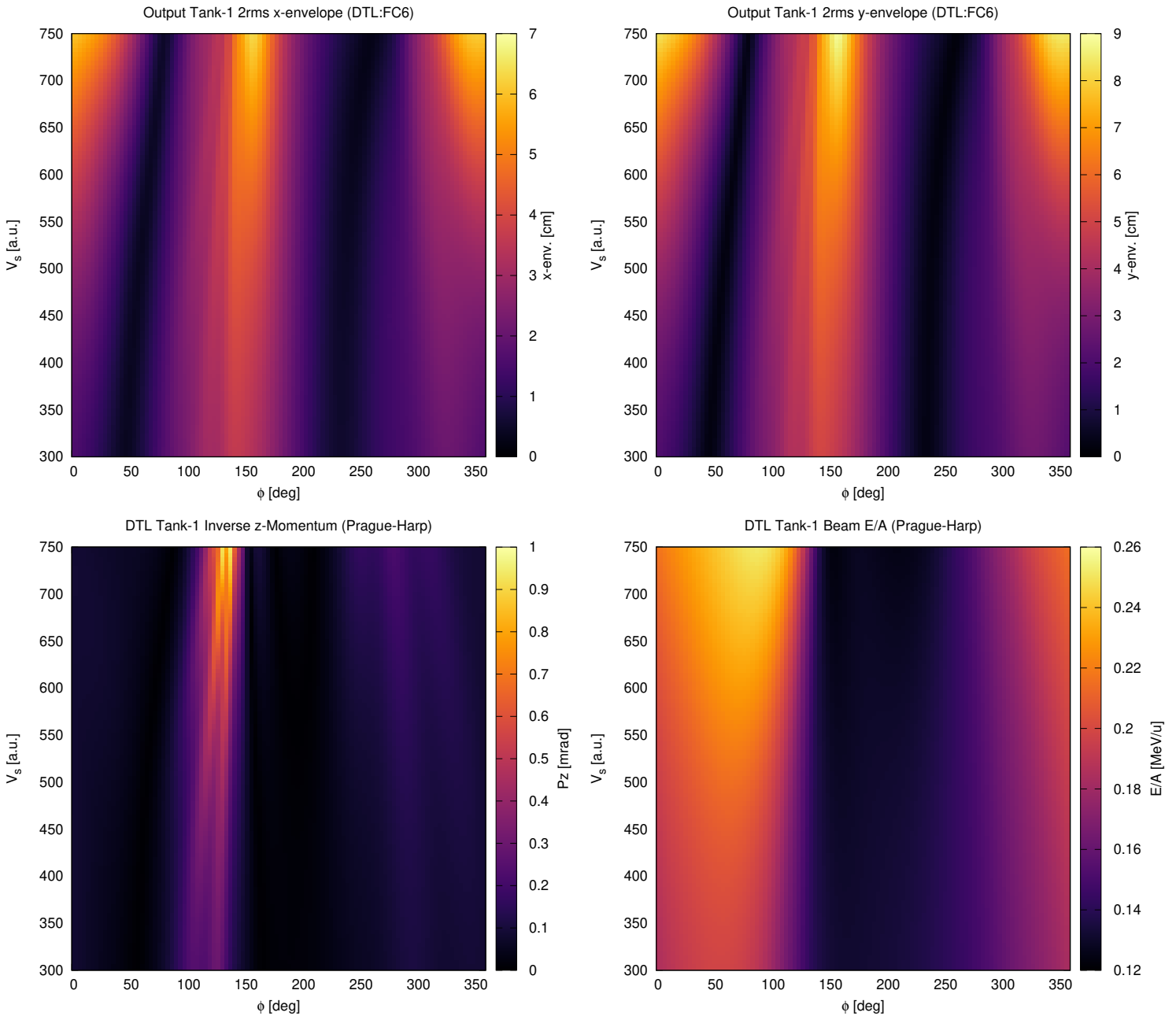


Figure 7: TRANSOPTR grid scans for quadrupole-free DTL accelerated beam, corresponding to IH Tank-1. A beam of  $^{20}\text{Ne}^{4+}$  at out-of-rfq  $E/A = 0.153$  MeV/u has been used. The energy ramp can be seen in voltage phase configuration space as the  $(V_s, \phi)$  pairs which maximize the  $P_z^{-1}$  signal (minimum energy spread). Scan performed at location of DTL:FC6.

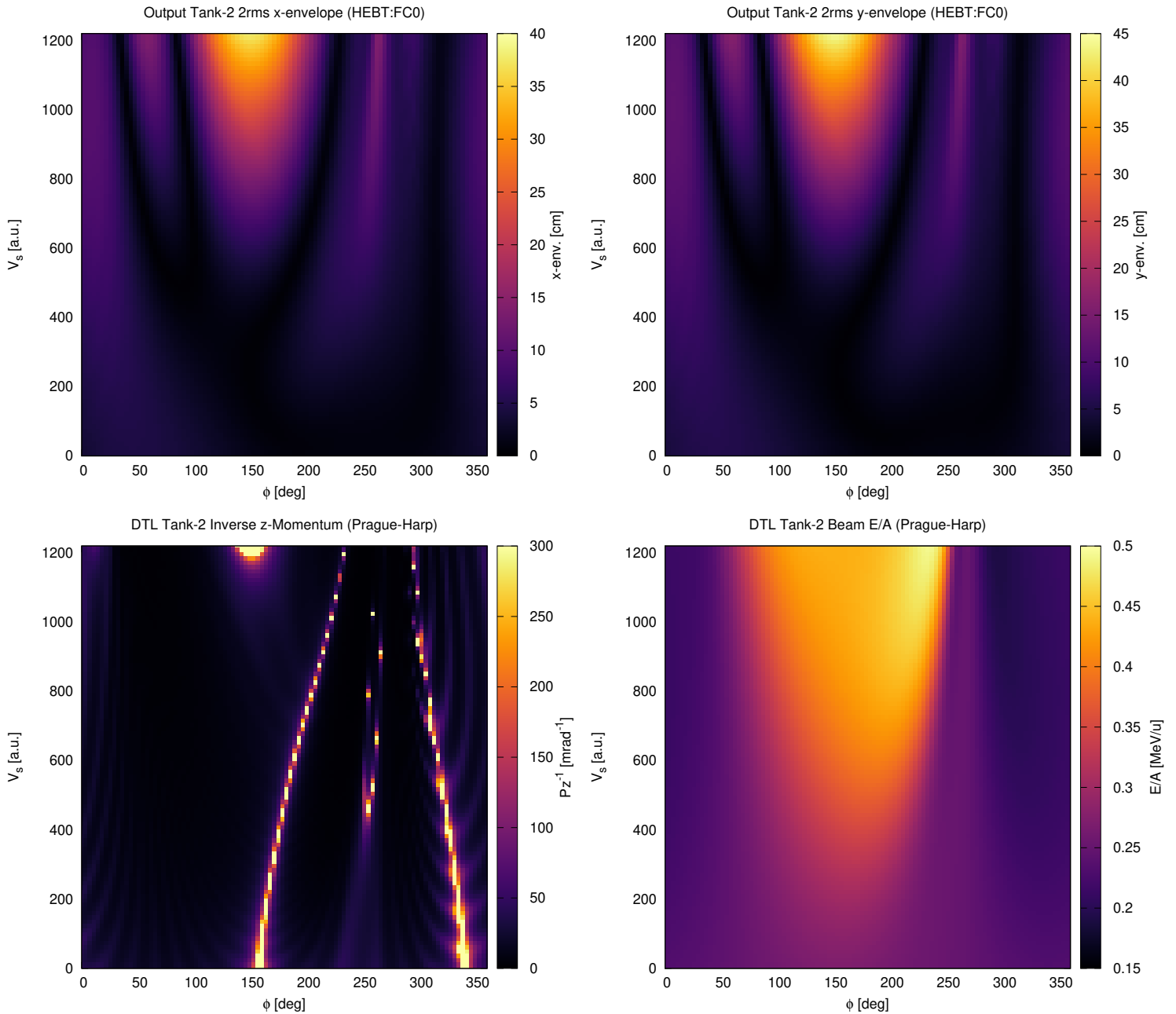


Figure 8: TRANSOPTR grid scans for quadrupole-free DTL accelerated beam, corresponding to IH Tank-2. A beam of  $^{20}\text{Ne}^{4+}$  at out-of-rfq  $E/A = 0.153$  MeV/u has been used. The energy ramp can be seen in voltage phase configuration space as the  $(V_s, \phi)$  pairs which maximize the  $P_z^{-1}$  signal (minimum energy spread). Scan performed at location of HEBT:FC0.

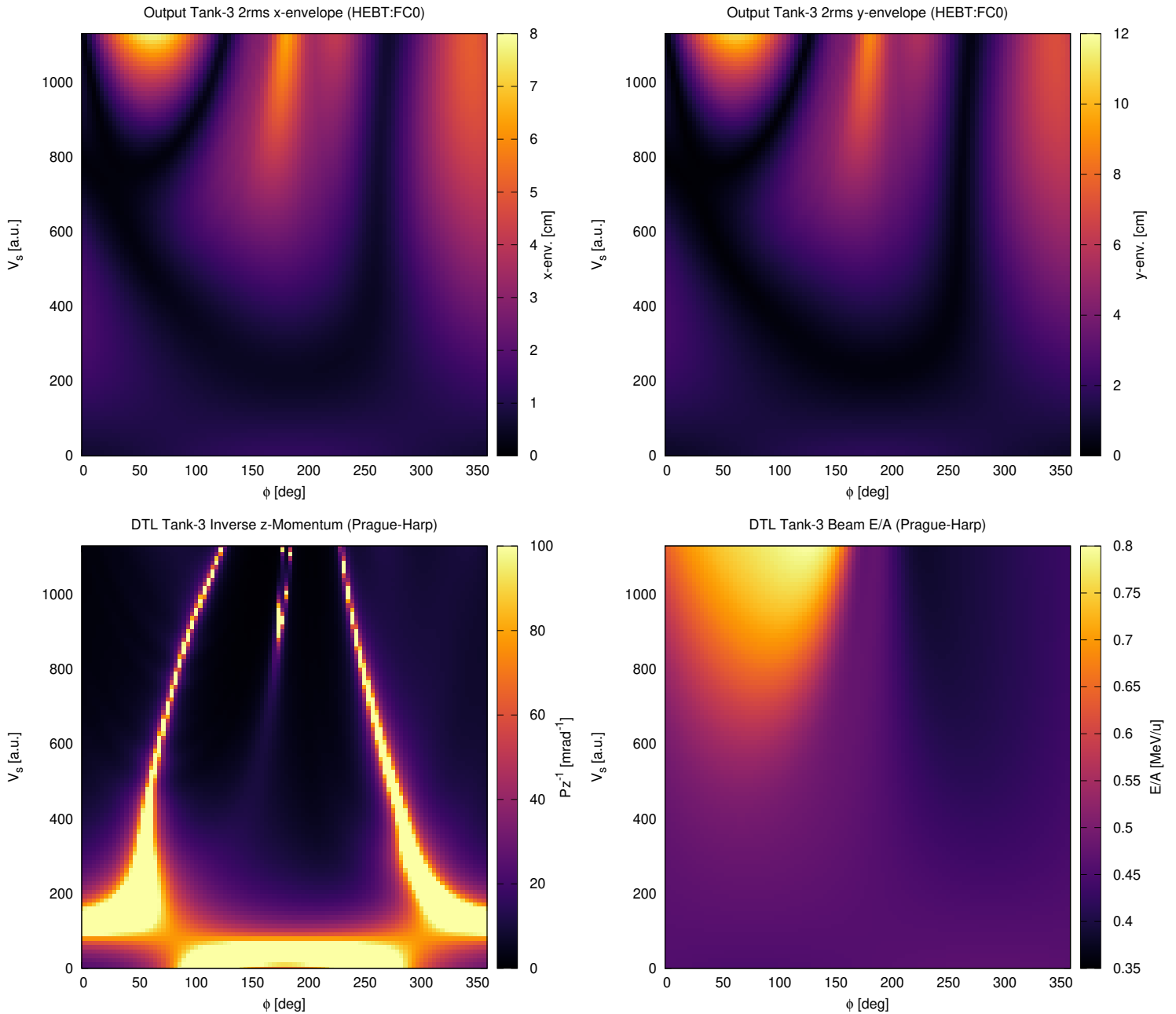


Figure 9: TRANSPORT grid scans for quadrupole-free DTL accelerated beam, corresponding to IH Tank-3. A beam of  $^{20}\text{Ne}^{4+}$  at out-of-rfq  $E/A = 0.153$  MeV/u has been used. The energy ramp can be seen in voltage phase configuration space as the  $(V_s, \phi)$  pairs which maximize the  $P_z^{-1}$  signal (minimum energy spread). Scan performed at location of HEBT:FC0.

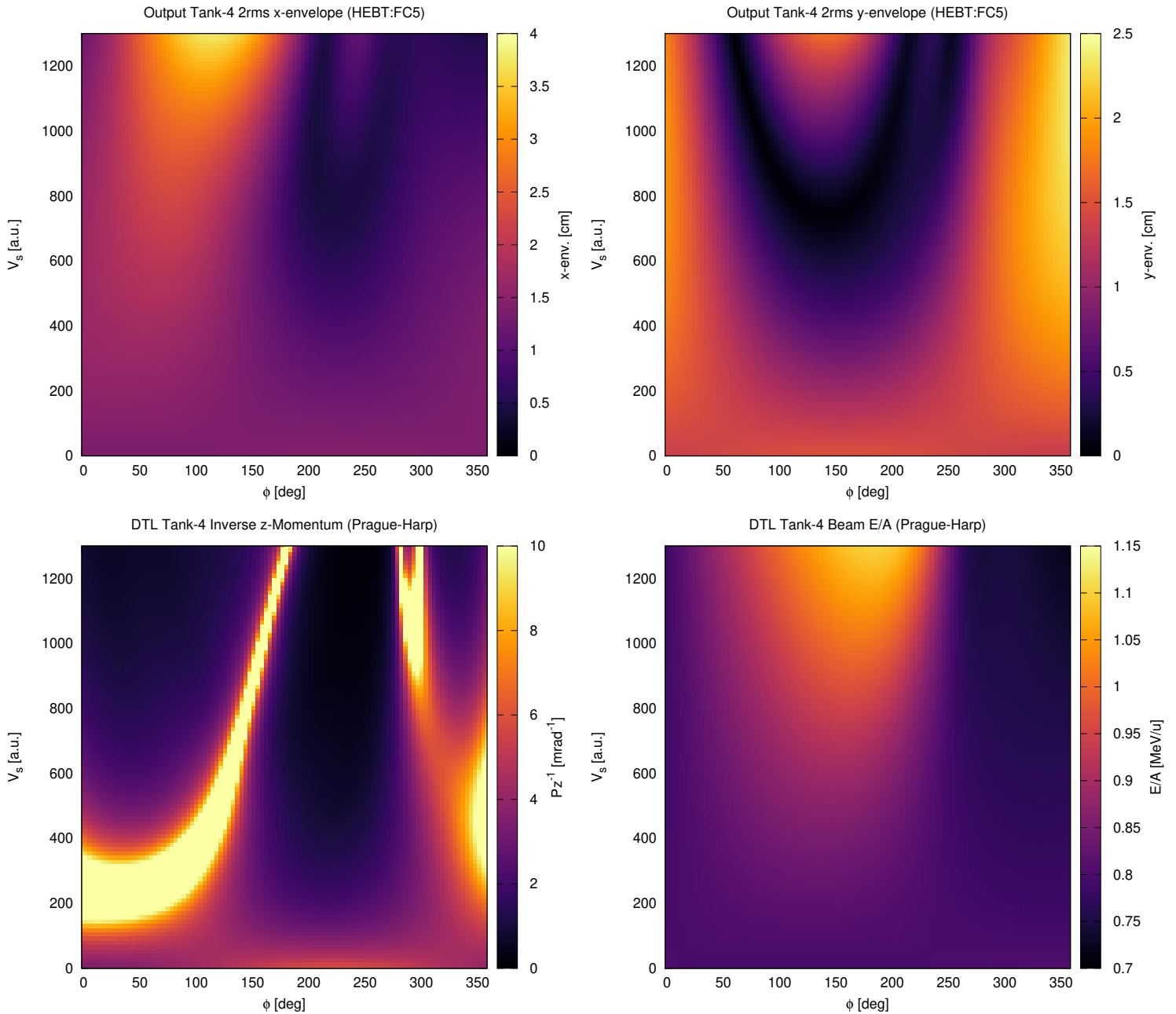


Figure 10: TRANSPORT grid scans for quadrupole-free DTL accelerated beam, corresponding to IH Tank-4. A beam of  $^{20}\text{Ne}^{4+}$  at out-of-rfq  $E/A = 0.153$  MeV/u has been used. The energy ramp can be seen in voltage phase configuration space as the  $(V_s, \phi)$  pairs which maximize the  $P_z^{-1}$  signal (minimum energy spread). Scan performed at location of HEBT:FC5.

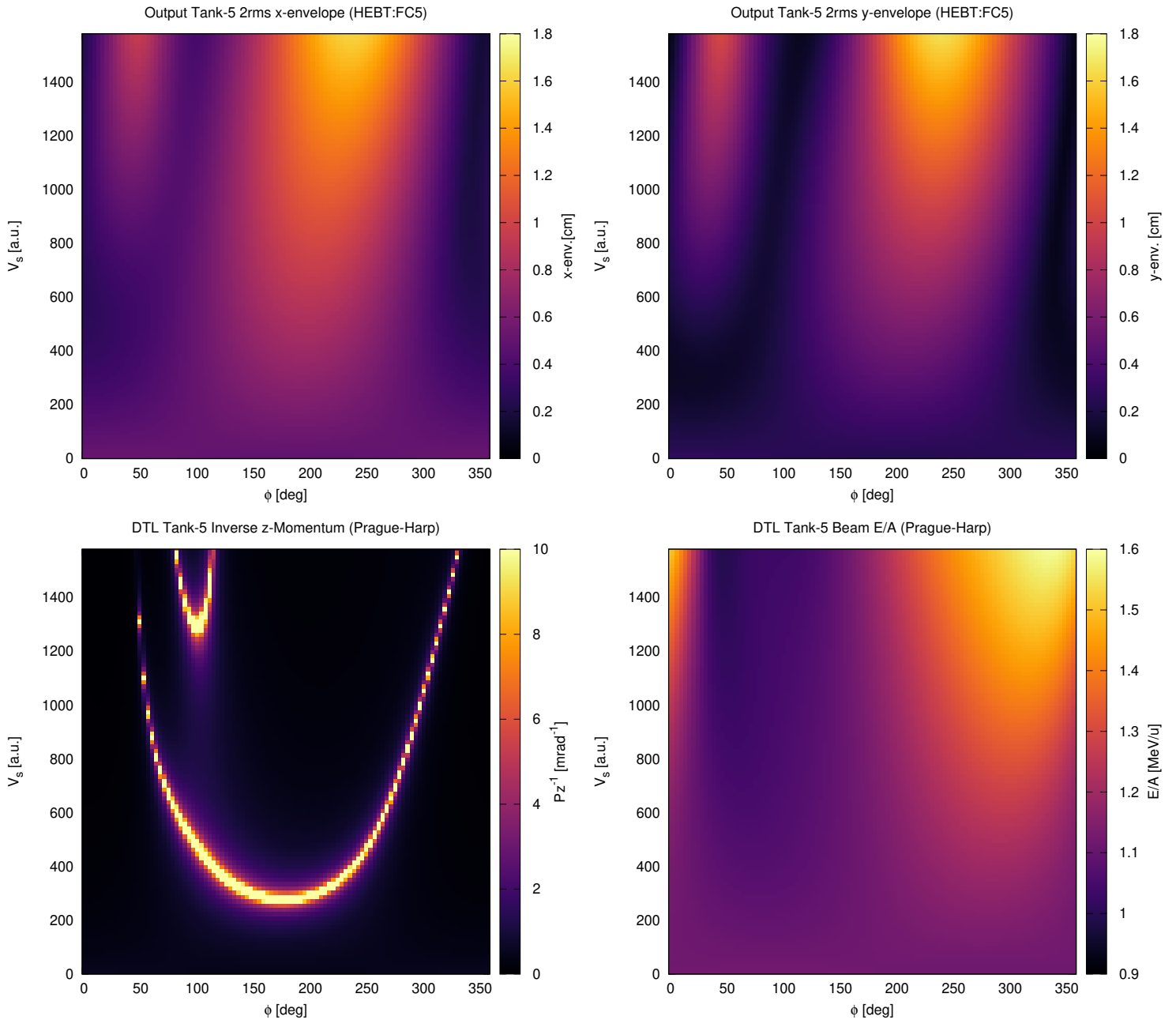


Figure 11: TRANSOPTTR grid scans for quadrupole-free DTL accelerated beam, corresponding to IH Tank-5. A beam of  $^{20}\text{Ne}^{4+}$  at out-of-rfq  $E/A = 0.153$  MeV/u has been used. The energy ramp can be seen in voltage phase configuration space as the  $(V_s, \phi)$  pairs which maximize the  $P_z^{-1}$  signal (minimum energy spread). Scan performed at location of HEBT:FC5.